CHAPTER-2

Metal-Organic Framework Derived Hollow Cobalt Vanadium Layered Double Hydroxide Nanocages for Efficient Electrochemical Water Oxidation

In this chapter, we have synthesized noble-metal-free V-doped Co-LDH (V_xCo-LDH) hollow nanocages using ZIF-67 as a precursor. The conversion of ZIF-67 into LDH, incorporating vanadium through treatment with VCl_3, was achieved. Vanadium doping was found to be essential for enhancing the OER activity of Co-LDH in an alkaline medium. We also investigated the effect of varying vanadium content on the activity of V_xCo-LDH and found that all V_xCo-LDH samples exhibited superior OER activity compared to Co-LDH, with $V_{0.2}$Co-LDH demonstrating the best performance. $V_{0.2}$Co-LDH required only 280 mV of overpotential to achieve a current density of 100 mA cm^{-2}, maintaining stability for 24 hours.

2.1. Introduction

It is a significant challenge to develop efficient, stable, and non-precious metal-based electrocatalysts for large-scale electrochemical water oxidation.[1][2] As mentioned in previous chapter, transition metal-based catalysts (including Fe, Mn, Co, and Ni) have garnered considerable attention due to their abundance, improved stability, and inherent activity.[3][4] Among various transition metal-based electrocatalysts, layered double hydroxides have been extensively studied as OER electrocatalysts.[5][6] [7] However, the major shortcomings of non-noble metal-based hydroxides and oxides is their limited catalytic activity, which is impeded by poor conductivity and structural limitations.[8] Therefore, further attempts are necessary to promote their activity by increasing the number of surface active sites and improving conductivity. Hollow nanostructured materials have been studied to improve water electrolysis performance because of their benefits, including a large exposed surface area for easy contact between the electrolyte and active sites, short pathways for charge and mass transport, and reduced diffusion blockage for smooth gas release at high current densities.[9][10][11]

Furthermore, doping metals and nonmetals has been effective in enhancing water oxidation by improving catalytic activity through structural transformations. [12][13][14] This provides abundant active metal sites that facilitate faster charge transport and ensure excellent electrical conductivity.[15]

As an early transition metal, vanadium possesses a broad range of oxidation states. This characteristic enables various adjustments to the electronic structure of materials, thereby improving their catalytic performance.[7],[16],[17] Vanadium-based catalysts, with their adaptable redox chemistry and abundant, affordable availability on Earth, present a viable alternative to the scarce and costly noble metals used in water splitting.[18][19] Angnes et al. provided an extensive

review of the advancements in NiV-LDHs as electrocatalysts for water splitting, emphasizing their significant potential in both HER and OER.[20] Similarly, Yang et al. developed vanadium-doped ultrathin and amorphous CoOOH which required only 250 mV of overpotential to generate 10 mA cm^{-2} current density.[21] In this reference, Sun et al. synthesized monolayered NiV-LDH that demonstrated excellent OER performance due to their improved conductivity, efficient electron transfer, and numerous active sites. This research has the potential to expand the variety of cost-effective electrocatalysts available for water splitting.[21][22] However, the OER activity of V-based LDHs is constrained as it undergo aggregation resulting in the limited use of active sites.[23] In this context, the use of ZIF-67 as sacrificial template can improvise the OER activity of V-based LDHs.[24]

Herein, we have reported the synthesis of a hierarchical hollow vanadium doped-Co layered double hydroxide (LDH) nanocages from ZIF-67 (zeolitic imidazolate framework) using a facile synthetic approach (Figure 1). The formation of V_xCo-LDH hollow nanocages is confirmed by PXRD, spectroscopic and microscopic techniques. The as-synthesized catalyst is employed for the alkaline electrochemical water oxidation to achieve excellent activity. It is observed that vanadium incorporation improves water oxidation activity by tuning the electronic structure of the catalysts and helping the Co centres to reach a high oxidation state.

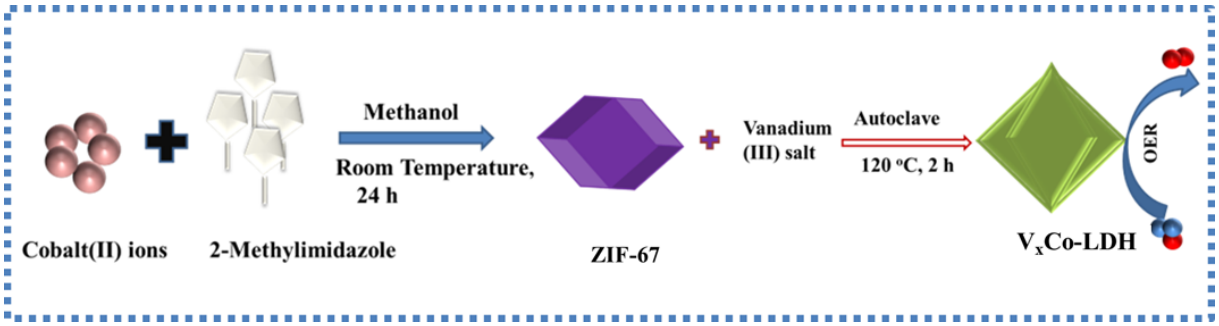

Scheme 2.1. Illustrative diagram depicting the synthesis of V-Co-LDH starting from ZIF-67

2.2. Chemicals

Cobalt nitrate hexahydrate was purchased from Sigma Aldrich (99.9%). Urea (99.5%) and ammonium fluoride (98%), ferric nitrate nonahydrate, 2-methyl imidazole were bought from SRL, India. All chemicals were used without any further purification. Nickel foam was purchased from AXYS technology, India. Double distilled water was used for all the experiments and electrochemical measurements.

2.3. Instruments

The crystallinity and phase identification of the synthesized catalysts were confirmed by room temperature X-ray diffraction (Rigaku Miniflex 600) using Cu-K alpha radiation (λ=1.5418 Å). The IR spectra were recorded at Nicolet iS5 FTIR spectrometer in attenuated total reflection (ATR) mode in the range between 400- 4000 cm^{-1}. The XPS has been measured using a Thermo Fisher Scientific instrument with Al K-alpha radiation operated at 150 W. Microstructure and compositional analyses of the prepared materials were examined with the help of Field emission scanning electron microscopy (Nova Nano SEM 450) equipped with an EDS System and the interlayer d-spacing of the synthesized catalysts was obtained by taking HR-TEM images (FEI TECNAI G2 20 TWIN) operated at 300 kV.

2.4 Experimental

2.4.1. Synthesis of ZIF-67

1 mmol of $Co(NO_3)_3.6H_2O$ was dissolved in 10 mL of methanol to get solution A. (4 mmol) 2-methylimidazole was dissolved in 20 mL methanol and stirred for 10 minutes to get solution B. Further, solution B was added dropwise in solution A with stirring. The as obtained reaction mixture was kept at room temperature for 12 h. After 12 hours, the ZIF-67 precipitate was collected

via centrifugation and subsequently washed with methanol. After that precipitate was dried at 60 ^{o}C overnight.[25]

2.4.2. Synthesis of V_xCo-LDH

100 mg of ZIF-67 was dispersed in 12.5 mL of ethanol. 20 mg of VCl_3 was dissolved in another 12.5 mL of ethanol. Solution of VCl_3 was added to the dispersion of ZIF-67 with simultaneous stirring. The as obtained reaction mixture was transferred in a Teflon cup and placed in an autoclave. The autoclave was sealed and heated in an electric oven at 120 ^{o}C for 2 h. After natural cooling down to room temperature, precipitates of V_xCo-LDH were collected by centrifugation at 14000 rpm and washed five times with methanol. After that precipitate was dried at 60 ^{o}C overnight.

2.4. 3. Activation of nickel foam

The activation of nickel foam refers to the cleaning of the surface by removing the inert oxide layers and other remnants to enhance the deposition of electrocatalysts.[26][27]

A piece of nickel foam (1 cm x 2 cm) was first washed with 3.0 M HCl under ultrasonication, followed by washing with water and ethanol repeatedly. The activated nickel foam was dried in an air oven for 12 h at 50 ^{o}C for further use.

2.4.4. Deposition of catalysts on nickel foam

As synthesized electrocatalysts were deposited on nickel foam by electrophoretic deposition (EPD) method. For EPD, first of all 3 mg of the as synthesized catalysts was dispersed in 15 mL of acetone along with 1 mg of iodine. After that, two activated nickel foams (1cm x 2 cm) were dipped into the solution containing catalysts. With Applied potential of 9.0 volt for three minutes, dispersed particles of catalysts got deposited on nickel foam. The catalyst-deposited nickel foam was dried and used for further measurements.[28]

2.5. Results and discussion

2.5.1. Characterizations of the catalysts

The catalyst precursor ZIF-67 was synthesized by solvothermal method by treating solution of cobalt nitrate hexahydrate in methanol with solution of 2-methylimidazole in methanol as shown in (**Scheme 2.1**). The XRD patterns of ZIF-67 demonstrated a good agreement in terms of relative intensity and peak positions with the ZIF-67 found in previous literature, indicating that ZIF-67 was successfully synthesized (JCPDS: 08-60-513, **Figure 2.1a**).[25]

After that, ZIF-67 was reacted with different amounts of V^{III}-salt to synthesize V_xCo-LDH **(Scheme 2.1 and Table 2.1)**.

Table 2.1. Details of various synthesized V_xCo-LDH catalysts

Catalyst	Precursor	Amount of salt used for LDH formation
Co-LDH	ZIF-67 (100mg)	$CoCl_2.6H_2O$ (0.2 mmol)
$V_{0.05}$-Co-LDH	ZIF-67 (100 mg)	VCl_3 (0.05 mmol)
$V_{0.1}$-Co-LDH	ZIF-67 (100 mg)	VCl_3 (0.1 mmol)
$V_{0.15}$-Co-LDH	ZIF-67 (100 mg)	VCl_3 (0.15 mmol)
$V_{0.2}$-Co-LDH	ZIF-67 (100 mg)	VCl_3 (0.2 mmol)
$V_{0.25}$-Co-LDH	ZIF-67 (100 mg)	VCl_3 (0.25 mmol)

Since the $V_{0.2}$Co-LDH catalyst showed the best OER activity therefore an extensive characterization was conducted for the same. The PXRD (powder X-ray diffraction pattern) of the catalyst $V_{0.2}$-Co-LDH demonstrated the peaks situated at 11.6°, 23.2°, 34.5°, 39.1°, 46.5°, 59.9°, and 60.9° corresponding to the (003), (006), (012), (015), (018), (110), and (013) respectively

(JCPDS No. 50-235) **(Figure 2.1a)**. [29]

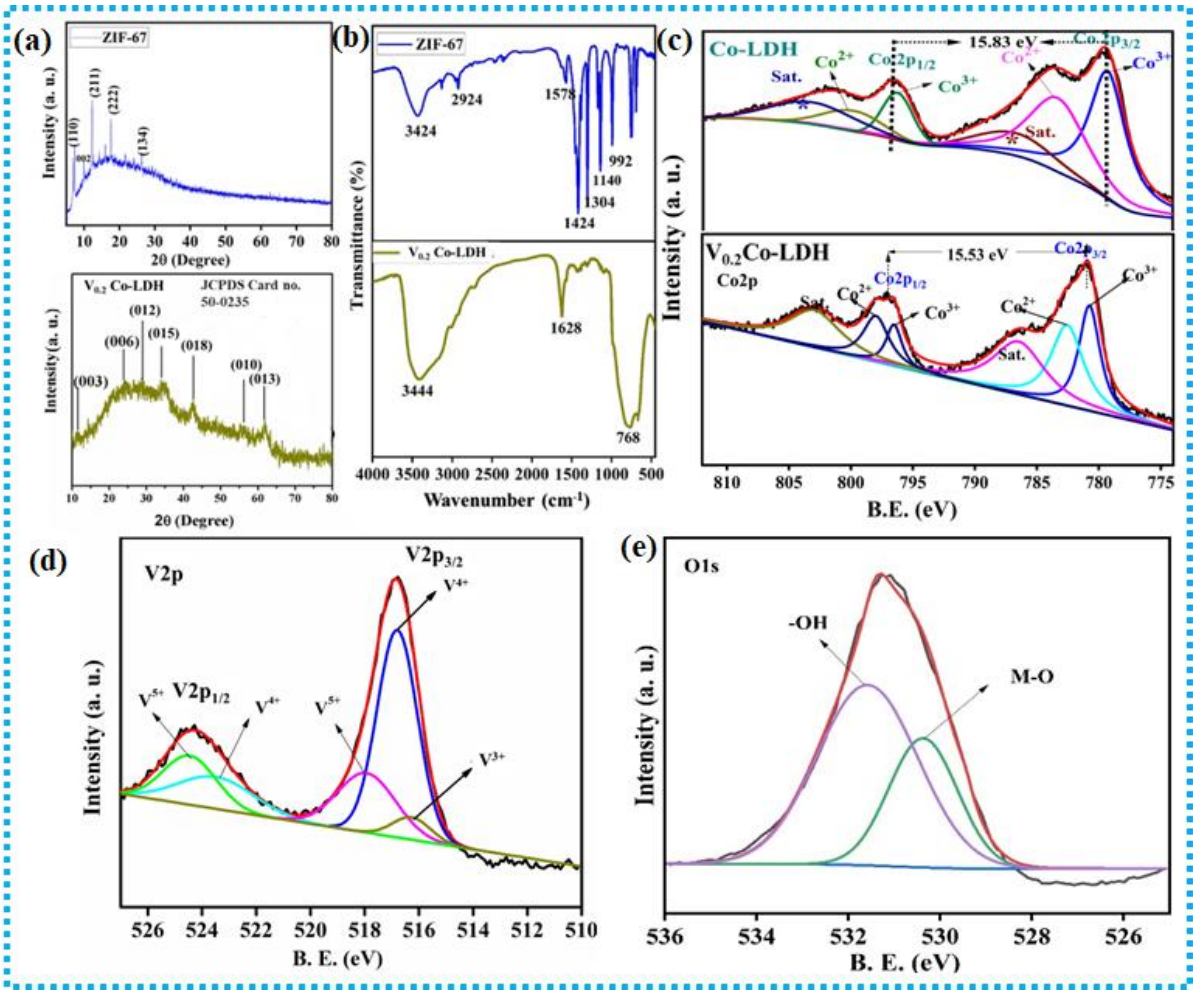

Figure 2.1. (a) The PXRD graph of ZIF-67 and $V_{0.2}$Co-LDH; (b) shows the FTIR spectra of ZIF-67 and $V_{0.2}$Co-LD; (c) The Co 2p XPS spectra of Co-LDH and $V_{0.2}$Co-LDH representing the tuning of the electronic structure by the introduction of V in the structure of the catalyst. The * marked peaks are satellite peaks of Co(II); (d) V 2p X-ray photoelectron spectrum of $V_{0.2}$Co-LDH. The V2p spectrum was deconvoluted into two peaks with binding energy 518.8 eV and 524.24 eV corresponding to V $2p_{1/2}$ andV $2p_{3/2}$ (e) The O 1s XPS was fitted into two peaks for the oxygen of -OH group, and Co/V-O bond.

The peak obtained at 1628 cm^{-1} in (FTIR) spectroscopy revealed the presence of CO_3^{2-} anions which were intercalated between the layers of metal hydroxide to balance its positive charge **(Figure 2.1b)**.[30] Furthermore, X-ray photoelectron spectroscopy (XPS) was performed to look

into the composition and surface chemical state of the as-synthesized catalysts $V_{0.2}$Co-LDH. The Co 2p spectrum, shows two pairs of spin–orbit doublets that correspond to the coexistence of Co^{2+} and Co^{3+}. The binding energies at 781.07 eV and 796.5 eV are corresponding to Co $2p_{3/2}$ and Co $2p_{1/2}$ of Co^{3+}, while those at 782.46 eV and 798.01 eV are related to Co^{2+} **(Figure 2.1c)**. The Co 2p XPS spectra was compared with Co 2p spectra of Co-LDH and it was observed that introduction of V into Co-LDH results in shifting of peak related to Co $2p_{3/2}$ by 0.65 eV and also the coupling spacing between Co $2p_{3/2}$-Co $2p_{1/2}$ spin-orbit was found to decreased from 15.83 eV (in Co-LDH) to 15.53 eV (in $V_{0.2}$Co-LDH) which clearly indicated a higher concentration of Co^{3+} in $V_{0.2}$Co-LDH compared to Co-LDH.[30][31] V 2p XPS spectrum was deconvoluted into V $2p_{3/2}$ and V $2p_{1/2}$ exhibiting the presence of peaks for V^{3+}, V^{4+}, and V^{5+} located at 516.09 eV, 516.8 eV and 517.8 eV respectively **(Figure 2.1d)**.[32][33]

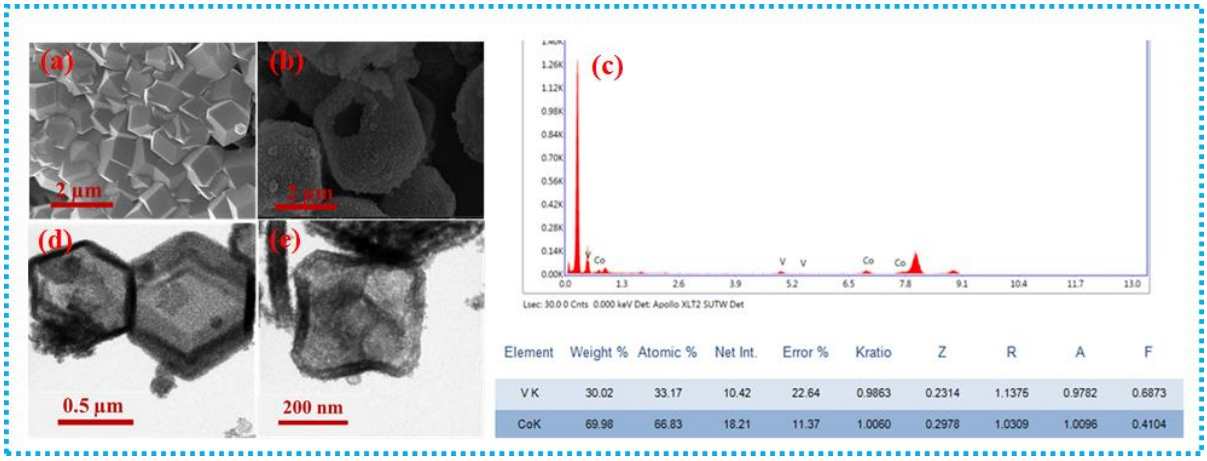

Figure 2.2. (a-b) SEM image of ZIF-67 and $V_{0.2}$Co-LDH; (b) TEM image showing the hollow nanocages of $V_{0.2}$Co-LDH; (c) EDX of the catalyst showing presence of Co, V and O; (d-e) TEM images of $V_{0.2}$Co-LDH.

The O 1s XPS spectra, demonstrated presence of 529.9 eV, and 528.45 eV belong to -OH group and oxide/hydroxide group **(Figure 2.1e)**.[21]

Scanning electron microscopy (SEM) images demonstrates the hollow nanocages morphology of

$V_{0.2}$Co-LDH **(Figure 2.2b)**. Furthermore, the dodecahedron morphology of ZIF-67 was completely destroyed after the treatment of VCl_3 **(Figure 2.2a)**. EDX characterization exhibited the presence of all elements Co, V, and O **(Figure 2.2 c)**. TEM image also confirmed the hollow morphology of the as synthesized catalyst $V_{0.2}$ Co-LDH **(Figure 2.2d-e)**.

2.5.2. Electrochemical activity

The electrocatalytic performance of $V_{0.2}$Co-LDH and other synthesized catalysts was evaluated using a three-electrode system with a scan rate of 5 mV s^{-1} in a 1.0 M aqueous KOH solution. Linear sweep voltammetry (LSV) polarization curves indicated that $V_{0.2}$Co-LDH demonstrated the highest OER activity among the synthesized catalysts **(Figure 2.3a)**. Each V_xCo-LDH catalyst exhibited higher OER activity than Co-LDH, unrevealing the significant impact of adding vanadium to Co-LDH. Additionally, varying the amount of V in V_xCo-LDH significantly influenced the OER activity, with a wide range of overpotentials observed, from 280 mV to 480 mV at a current density of 100 mA cm^{-2} **(Figure 2.3c)**. Increasing the amount of V in Co-LDH lowered the overpotential, reaching an optimal value for $V_{0.2}$Co-LDH. Beyond this point, further increases in V content caused the overpotential to rise **(Figure 2.3c)**. $V_{0.2}$Co-LDH required the overpotential 280 mV to produce the current density of 100 mA cm^{-2} which is remarkably lower than that of Co-LDH (450 mV). Actually, the OER overpotential obtained for $V_{0.2}$Co-LDH is higher than the vanadium doped LDH catalysts reported in the literature **(Table 2.2)**.

Tafel analysis was used to assess the kinetics of the OER with the produced catalysts under semi-stationary circumstances **(Figure 2.3b-c)**. $V_{0.2}$Co-LDH was found to have the lowest Tafel slope (59 mV $dec^{-1)}$ indicating quicker OER kinetics. Furthermore, the comparative assessment of the Tafel slope across catalysts with varying amounts of V indicated that $V_{0.2}$Co-LDH demonstrated remarkably vary small value for Tafel slope among all V_xCo-LDH catalysts.

Furthermore, electrochemical characterizations, including electronic impedance spectroscopy (EIS) and double-layer capacitance measurements, demonstrated the enhanced OER activity of $V_{0.2}$Co-LDH compared to Co-LDH. The impedance spectra revealed a significant reduction in charge transfer resistance (R_{ct}) upon the addition of V in the structure of Co-LDH **(Figure 2.3e).** $V_{0.2}$Co-LDH had the quickest charge transfer kinetics of all the catalysts, as evidenced by the smallest R_{ct} value of 1.65 Ω.

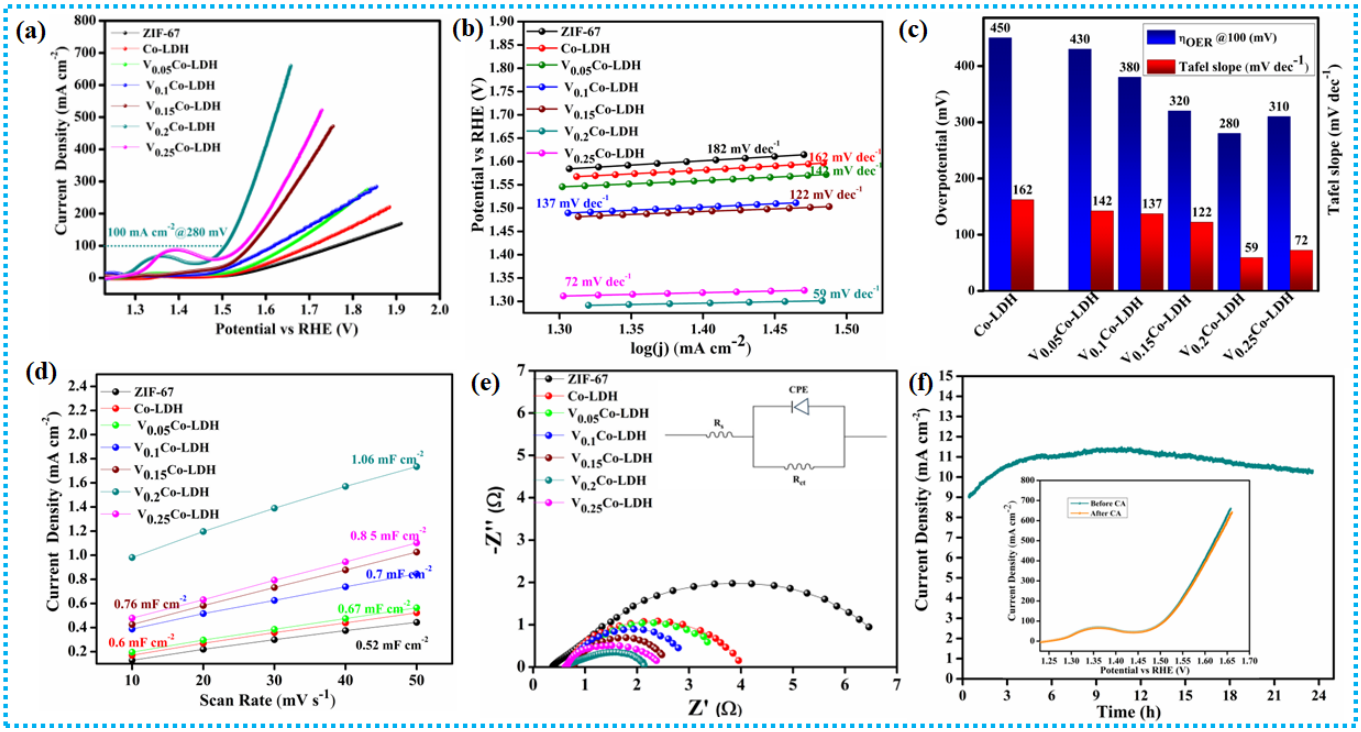

Figure 2.3. (a) LSV profiles for OER of V_xCo-LDH catalysts having different amount of V in the structure**;** (b) Tafel plots for the oxygen evolution reaction of $V_{0.2}$Co-LDH compared with other catalysts; The lowest Tafel slope for $V_{0.2}$Co-LDH was observed; (c)comparative plots of the overpotentials and Tafel slopes for the catalysts showing the best activity and fastest kinetics for $V_{0.2}$Co-LDH; (d) Determination of double-layer capacitance (C_{dl}) of the as synthesized catalysts; (e) demonstrates Nyquist plots for the catalysts, obtained from electrochemical impedance spectroscopic (EIS) measurements showing lowest charge transfer resistance for $V_{0.2}$Co-LDH; (f) chronoamperometric stability test of $V_{0.2}$Co-LDH and inset showing negligible change in the LSV profile after a 24 h long high current density chronoamperometric study.

In OER catalysis, the active surface area is a key factor for catalytic activity. We estimated the electrochemically active surface areas (ECSAs) of the catalysts by measuring their double-layer capacitances (C_{dl}).[34] $V_{0.2}$Co-LDH stands out among the catalysts with the highest C_{dl} value, indicating the largest ECSA **(Figure 2.3d)**.

The enhanced OER performance of $V_{0.2}$Co-LDH is attributed to the high-valence V^{4+}/V^{5+} ions, which attract electrons to maintain the neighbouring Co ions in a high-valence state, thereby accelerating the OER process.[35][36]

Table 2.2. The OER activities of reported LDHs compared with $V_{0.2}$Co-LDH.

Sr. No.	Catalyst	Current density ($mA\ cm^{-2}$)	Overpotential (mV)	Reference
1	$V_{0.2}$Co-LDH	100	280	This work
2	CoFeV LDH/NF	10	242	[37]
3	CoV-LDHs@FeOOH/NF	10	232	[23]
4	Se-NiV LDH	50	198	[38]
5	CoMoV-LDHs@NF	10	270	[39]
6	Fe-dopedNiVHMS	10	255	[40]
7	NiFeV LDHs	20	195	[41]
8	V-NiFe-LDH/NF	195	239	[42]
9	FeV/meso-Co	10	280	[43]
10	V–$Ni(OH)_2$/NF	100	275	[44]
11	NiCo-LDH hollow	100	303	[45]
12	NiCoV-LDH	10	280	[46]
13	CoFeV-LDH	10	376	[47]
14	CoFe-NiV-LDH	10	150	[48]
15	Ru@NiV-LDH	10	272	[49]
16	Ni_5P_4@FeV LDH	50	250	[50]
17	Ru- doped Co-V-LDH	10	230	[51]

The higher oxidation state of cobalt not only offers high conductivity, as shown by the EIS results in **(Figure 2.3e)** but also functions as the true active sites in OER catalysis. Moreover, as formed hierarchical hollow structure increases both surface area and active site exposure, facilitating the

rapid release of bubbles.[52]

Moreover, durability is a crucial factor in the practical application of electrocatalysts. The stability of $V_{0.2}$Co-LDH was assessed using chronoamperometric (CA) measurements at an overpotential of 1.5 V **(Figure. 2.3f)**. $V_{0.2}$Co-LDH produced oxygen continuously for 24 hours while displaying a constant current density. After 24 h of CA measurement, the acquired LSV data demonstrated slightly decrease in the activity **(inset, Figure 2.3)**, indicating the stability of $V_{0.2}$Co-LDH.

2.6. Conclusion

In summary, we prepared V-doped Co- layered double hydroxide with hollow nanostructure morphology, using ZIF-67 as precursor to serve as OER catalyst. The optimum incorporation of V in Co-LDH structure result in the enhanced OER activity. Incorporating V was observed to alter the morphology of the resulting nanosheets, providing a high ECSA for electrocatalysis and at the same time it also modulated the electronic structure of Co-LDH leading to the optimized absorption strength of *O intermediates thereby facilitating the OER process.

2.7. References

[1] A. Indra, U. Paik, T. Song, *Angew. Chemie - Int. Ed.* **2018**, *57*, 1241.

[2] Q. Liu, J. Huang, Y. Zhao, L. Cao, K. Li, N. Zhang, D. Yang, L. Feng, L. Feng, *Nanoscale* **2019**, *11*, 8855.

[3] X. Bo, Y. Li, X. Chen, C. Zhao, *Chem. Mater.* **2020**, *32*, 4303.

[4] B. H. R. Suryanto, Y. Wang, R. K. Hocking, W. Adamson, C. Zhao, *Nat. Commun.* **2019**, *10*, 13415.

[5] C. Wu, M. Zhong, Y. Tan, *Chem. Eng. J.* **2023**, *477*, 146981.

[6] H. Shi, H. Liang, F. Ming, Z. Wang, *Angew. Chemie* **2017**, *129*, 588.

[7] W. Zhang, L. Cui, J. Liu, *J. Alloys Compd.* **2020**, *821*, 153542.

[8] S. H. Ye, Z. X. Shi, J. X. Feng, Y. X. Tong, G. R. Li, *Angew. Chemie - Int. Ed.* **2018**, *57*, 2672.

[9] J. Zhang, L. Yu, Y. Chen, X. F. Lu, S. Gao, X. W. Lou, *Adv. Mater.* **2020**, *32*, 1906432.

[10] J. He, Y. Chen, A. Manthiram, *Energy Environ. Sci.* **2018**, *11*, 2560.

[11] X. Zhang, C. Li, T. Si, H. Lei, C. Wei, Y. Sun, T. Zhan, Q. Liu, J. Guo, *ACS Sustain. Chem. Eng.* **2018**, *6*, 8266.

[12] J. Feng, X. Wang, D. Zhang, Y. Wang, J. Wang, M. Pi, H. Zhou, J. Li, S. Chen, *J. Electrochem. Soc.* **2018**, *165*, F1323.

[13] C. Xiao, Y. Li, X. Lu, C. Zhao, *Adv. Funct. Mater.* **2016**, *26*, 3515.

[14] X. Luo, P. Ji, P. Wang, R. Cheng, D. Chen, C. Lin, J. Zhang, J. He, Z. Shi, N. Li, S. Xiao, S. Mu, *Adv. Energy Mater.* **2020**, *10*, 1903891.

[15] L. Wang, Y. Li, Q. Sun, Q. Qiang, Y. Shen, Y. Ma, Z. Wang, C. Zhao, *ChemCatChem* **2019**, *11*, 2011.

[16] M. A. Ehsan, A. Khan, A. Al-Ahmed, A. S. Hakeem, M. Afzaal, S. Pandey, N. Mahar, *Int. J. Hydrogen Energy* **2024**, *52*, 718.

[17] M. Kashif, S. Thangarasu, N. Murugan, S. S. Magdum, Y. A. Kim, M. Kurkuri, T. H. Oh, *J. Energy Storage* **2024**, *81*, 110348.

[18] C. Wu, M. Zhong, Y. Tan, *Chem. Eng. J.* **2023**, *477*, 146981.

[19] Y. Ma, M. X. Li, R. N. Luan, C. R. Li, X. Liu, H. Y. Zhao, Y. H. Wang, Y. M. Chai, B. Dong, *Int. J. Hydrogen Energy* **2022**, *47*, 33352.

[20] J. M. Gonçalves, P. R. Martins, K. Araki, L. Angnes, *J. Energy Chem.* **2021**, *57*, 496.

[21] J. Liu, Y. Ji, J. Nai, X. Niu, Y. Luo, L. Guo, S. Yang, *Energy Environ. Sci.* **2018**, *11*, 1736.

[22] K. Fan, H. Chen, Y. Ji, H. Huang, P. M. Claesson, Q. Daniel, B. Philippe, H. Rensmo, F. Li, Y. Luo, L. Sun, *Nat. Commun.* **2016**, *7*, 11981.

[23] Z. Wang, L. Chen, S. Xu, D. Zhang, X. Zhou, X. Wu, X. Xie, X. Qiu, *Compos. Commun.* **2021**, *27*, 100780.

[24] X. Liu, Y. Liu, Y. Li, J. Zhuang, J. Tang, *Electrochim. Acta* **2023**, *471*, 143347.

[25] Y. Zhang, Y. Jia, M. Li, L. Hou, *Sci. Rep.* **2018**, *8*, 9597.

[26] Y. Rao, Y. Wang, H. Ning, P. Li, M. Wu, *ACS Appl. Mater. Interfaces* **2016**, *8*, 33601.

[27] L. Jia, G. Du, D. Han, Y. Hao, W. Zhao, Y. Fan, Q. Su, S. Ding, B. Xu, *J. Mater. Chem. A* **2021**, *9*, 27639.

[28] A. A. Daryakenari, B. Mosallanejad, E. Zare, M. A. Daryakenari, A. Montazeri, A. Apostoluk, J. J. Delaunay, *Int. J. Hydrogen Energy* **2021**, *46*, 7263.

[29] Q. Dong, C. Shuai, Z. Mo, N. Liu, G. Liu, J. Wang, H. Pei, Q. Jia, W. Liu, X. Guo, *J. Solid State Chem.* **2021**, *296*, 121967.

[30] P. Maurya, V. Vyas, A. N. Singh, A. Indra, *Chem. Commun.* **2023**, 7200.

[31] B. Singh, A. K. Patel, A. Indra, *Mater. Today Chem.* **2022**, *25*, 100930.

[32] Y. Cui, Y. Xue, R. Zhang, J. Zhang, X. Li, X. Zhu, *J. Mater. Chem. A* **2019**, *7*, 21911.

[33] S. H. Hsu, S. F. Hung, H. Y. Wang, F. X. Xiao, L. Zhang, H. Yang, H. M. Chen, J. M. Lee, B. Liu, *Small Methods* **2018**, *2*, 1800001.

[34] F. Song, X. Hu, *J. Am. Chem. Soc.* **2014**, *136*, 16481.

[35] C. Jiang, J. Yang, T. Zhao, L. Xiong, Z. X. Guo, Y. Ren, H. Qi, A. Wang, J. Tang, *Appl. Catal. B Environ.* **2021**, *282*, 119571.

[36] C. Jiang, J. Yang, X. Han, H. Qi, M. Su, D. Zhao, L. Kang, X. Liu, J. Ye, J. Li, Z. X. Guo, N. Kaltsoyannis, A. Wang, J. Tang, *ACS Catal.* **2021**, *11*, 14884.

[37] Y. Hu, Z. Wang, W. Liu, L. Xu, M. Guan, Y. Huang, Y. Zhao, J. Bao, H. M. Li, *ACS Sustain. Chem. Eng.* **2019**, *7*, 16828.

[38] A. De, R. Madhu, K. Bera, H. N. Dhandapani, S. Nagappan, S. Singha Roy, S. Kundu, *J. Mater. Chem. A* **2023**, *11*, 25055.

[39] J. Bao, Z. Wang, J. Xie, L. Xu, F. Lei, M. Guan, Y. Zhao, Y. Huang, H. Li, *Chem. Commun.* **2019**, *55*, 3521.

[40] Y. Deng, Y. Lu, R. Dai, M. Xiang, Z. Zhang, X. Zhang, Q. Zhou, H. Gu, J. Bai, *J. Colloid Interface Sci.* **2022**, *627*, 215.

[41] P. Li, X. Duan, Y. Kuang, Y. Li, G. Zhang, W. Liu, X. Sun, *Adv. Energy Mater.* **2018**, *8*, 1703341.

[42] J. Liang, H. Shen, Y. Ma, D. Liu, M. Li, J. Kong, Y. Tang, S. Ding, *Dalt. Trans.* **2020**, *49*, 11217.

[43] M. S. Amer, P. Arunachalam, M. A. Ghanem, M. Al-Shalwi, A. Ahmad, A. I. Alharthi, A. M. Al-Mayouf, *Int. J. Energy Res.* **2021**, *45*, 9422.

[44] P. Zhao, L. Ma, J. Guo, *J. Phys. Chem. Solids* **2022**, *164*, 110634.

[45] X. Shi, J. Li, X. Zhang, J. Guo, *J. Phys. Chem. Solids* **2023**, *172*, 111051.

[46] K. Bera, A. Karmakar, S. Kumaravel, S. Sam Sankar, R. Madhu, H. N Dhandapani, S. Nagappan, S. Kundu, *Inorg. Chem.* **2022**, *61*, 4502.

[47] W. Adamson, C. Jia, Y. Li, C. Zhao, *Int. J. Hydrogen Energy* **2021**, *46*, 35230.

[48] G. Srividhya, T. Sangavi, C. Viswanathan, N. Ponpandian, *ACS Appl. Energy Mater.* **2024**, *7*, 154.

[49] A. Karmakar, K. Karthick, S. S. Sankar, S. Kumaravel, R. Madhu, K. Bera, H. N. Dhandapani, S. Nagappan, P. Murugan, S. Kundu, *J. Mater. Chem. A* **2022**, *10*, 3618.

[50] J. Guan, X. Li, Y. Zhu, Y. Dai, R. Zhang, B. Guo, M. Zhang, *New J. Chem.* **2023**, *47*, 16964.

[51] W. Li, B. Feng, L. Yi, J. Li, W. Hu, *ChemSusChem* **2021**, *14*, 730.

[52] X. Shi, J. Li, X. Zhang, J. Guo, *J. Phys. Chem. Solids* **2023**, *172*, 111051.